

Improvement of High-Voltage Electrochemical Performance of Surface Modified $\text{LiNi}_{0.6}\text{Co}_{0.2}\text{Mn}_{0.2}\text{O}_2$ Cathode by La_2O_3 Coating

Jianxiong Liu¹, Xiaodong Jiang¹, Yannan Zhang^{2,*}, Peng Dong^{2,*}, Jianguo Duan², Yingjie Zhang², Yunfeng Luo³, Zewei Fu³, Yuhan Yao¹, Chengyi Zhu¹, Xiaohua Yu^{1,4}, Zhaolin Zhan¹

¹ National and Local Joint Engineering Laboratory for Lithium-ion Batteries and Materials Preparation Technology, Key Laboratory of Advanced Battery Materials of Yunnan Province, Faculty of Materials Science and Engineering, Kunming University of Science and Technology, Kunming 650093, China

² National and Local Joint Engineering Laboratory for Lithium-ion Batteries and Materials Preparation Technology, Key Laboratory of Advanced Battery Materials of Yunnan Province, Faculty of Metallurgical and Energy Engineering, Kunming University of Science and Technology, Kunming 650093, China

³ Yunnan Tin Group (Holding) Company Limited, Kunming 650000, China

⁴ National Engineering Research Center of Waste Resource Recovery, Kunming University of Science and Technology, Kunming 650093, China

*E-mail: zyn_legolas@163.com, dongpeng2001@126.com

Received: 29 May 2018 / Accepted: 23 July 2018 / Published: 1 September 2018

Layered transition-metal oxides $\text{LiNi}_{0.6}\text{Co}_{0.2}\text{Mn}_{0.2}\text{O}_2$ (NCM 622) due to their poor stability when worked at high operating voltage have limited their applications in industry. In this study, La_2O_3 is coated on NCM 622 positive electrodes via a facile solvothermal method. The scanning electron microscopy (SEM) and EDS test results show that La_2O_3 nano-particles are successfully coated on the surface of NCM 622 samples. The favorable Li-ion conductivity of the La_2O_3 -modified NCM 622 sample lead to obvious improvement in its electrochemical performances. In particular, the coated sample exhibits a capacity retention over 80% at 1 C after 100 cycles at a high cut-off voltage of 4.5 V, while that of the bare electrode is less than 60%. The alternating current impedance and cyclic voltammetry (CV) tests show that the La_2O_3 coating can effectively restrain the electrode polarization and reduce the Li-ion charge transfer resistance of cathode materials.

Keywords: $\text{LiNi}_{0.6}\text{Co}_{0.2}\text{Mn}_{0.2}\text{O}_2$; Cathode; Coating, High cut-off voltage

1. INTRODUCTION

Lithium-ion batteries are widely used in electric vehicles (EV), hybrid electric vehicles (HEV) and other portable appliances for their advantages, such as high output power, low self-discharge rate,

long service life, and environmental friendliness [1-3]. Since the commercialization of lithium-ion batteries, LiCoO₂ has been applied to the positive of lithium-ion batteries because of its high cycling stability and low irreversible capacity loss. However, the problems of large toxicity, high cost, and poor cycling performance at high cut-off voltages restrict its further applications. Recently, some researchers are actively looking for other suitable lithium-ion battery positive materials [4,5]. The layered transition-metal oxides LiNi_{0.6}Co_{0.2}Mn_{0.2}O₂ (NCM 622) has good thermal stability, high voltage platform, high energy density, low toxicity and low cost, which is considered to be a ideal cathode material to replace LiCoO₂ [6]. However, because of adverse side reactions between the active material and the electrolyte, the NCM 622 is suffered from serious capacity fading at high cut-off voltages (above 4.3 V) or at high current conditions, and then resulting in poor cycling performance [7].

Surface coating is an effective measure to suppress side reactions between active materials and electrolytes [8-11]. Liu [12] et al. prepared Li₂Si₂O₅-coated NCM 622 cathode material by a solution method, which improved the cycling stability of the active material at high cut-off voltage (the capacity retention of 86.4% after 150 cycles at 4.5 V). Tao [13] et al. modified NCM 622 with ZrO₂ to increase the capacity retention of active material from 75.6% to 83.8% after 100 cycles. Qin [14] et al. used nano-TiO₂ to coat NCM 622 by atomic layer deposition (ALD) method, which improved the cycling stability of NCM 622 (capacity retention of 85.9% after 100 cycles). To our best knowledge, La₂O₃ is oxides of the lanthanide series with good high temperature resistance and anti-acid corrosion abilities. In addition, La₂O₃ shows favorable Li-ion conduction efficiency because it is a good lithium ion conducting medium [15-17]. In this work, The La₂O₃-coated NCM 622 positive material (NCM 622-L) is successfully synthesized via a facile solvothermal method. Moreover, we have also explored the structure, morphology, and the electrochemical performance of NCM 622 after La₂O₃ coating at high cut-off voltage of 4.5 V.

2. EXPERIMENTAL

2.1. Preparation

The co-precipitation method was used to prepare spherical Ni_{0.6}Co_{0.2}Mn_{0.2}(OH)₂ precursor. NiSO₄·6H₂O, CoSO₄·7H₂O and MnSO₄·H₂O were mixed in deionized water at a molar ratio (Ni: Co: Mn = 6:2:2). The reaction temperature was kept at 60°C and pH was controlled by NH₃·H₂O solution to 10-11. The resulting precipitate was washed with deionized water and dried in a vacuum oven for 12 h to synthesize Ni_{0.6}Co_{0.2}Mn_{0.2}(OH)₂ precursor. The Li₂CO₃ was uniformly mixed with Ni_{0.6}Co_{0.2}Mn_{0.2}(OH)₂ in accordance with (n (Li): n (Ni + Co + Mn) = 1.05: 1). The mixture microsphere was first heated at 500°C for 5 h, and then sintered at 900 °C for 12 h.

The La₂O₃-coated NCM 622 positive material was synthesized by solvothermal method. (La(NO₃)₃·6H₂O) was completely dissolved in 50 mL absolute ethanol. The NCM 622 powder was added into the above solution, and placed in a reaction kettle and heated in oil bath for 24 h at 120°C. After that, the resulting powder was dried in a vacuum drying oven for 12 h, and sintered in a vacuum

tube furnace for 6 h at 500°C to obtain a La₂O₃ coated NCM 622 sample (marked as NCM 622-L). The coating amount of La₂O₃ was 5 wt.% of the pristine NCM 622 powder. The experimental process is shown in Figure 1.

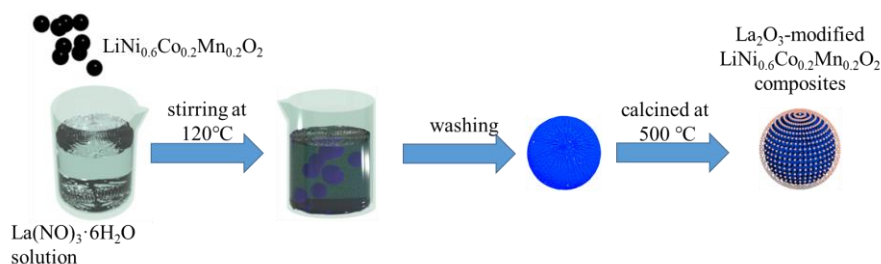


Figure 1. Coating process of LiNi_{0.6}Co_{0.2}Mn_{0.2}O₂ with La₂O₃

2.2. Characterization

The crystal structure of all the samples was characterized by a D/MAX-2200 X-ray diffractometer (XRD) using Cu K α radiation in the 2 θ range of 10–80° at a continuous scan mode with a step size of 0.02° and a scan rate of 10° min⁻¹. The microstructure of the samples before and after coating was characterized by JSM-5600LV scanning electron microscope (SEM). Energy Dispersive Spectrometry (EDS) was used to characterize the elemental species of the samples.

2.3. Electrochemical measurements

The active material was assembled into CR2032 coin cell (Shenzhen, Ming Ruixiang Co., Ltd.) in an argon-filled glove box for further electrochemical testing. The positive material that consisted of 80 wt.% of coated active materials, 10 wt.% of conductive acetylene black and 10 wt.% of polyvinylidene fluoride (PVDF) binder were dissolved in N-methyl-2-pyrrolidone (NMP) solvent. 1 M LiPF₆ dissolved in a 1:1:1 (v/v/v) ethylene carbonate (EC)/dimethyl carbonate (DMC)/ethyl methyl carbonate (EMC) was used as electrolyte. *Lithium metal was used as the negative electrode.* The charge/discharge performance test was performed between 3.0 and 4.5 V (vs. Li/Li⁺) at different scanning rate using the CT-3008 battery test system (Shenzhen Newware Electronics, Ltd.). In addition, the tests of cyclic voltammetry (CV) and electrochemical impedance (EIS) tests were carried out using an electrochemical workstation (CHI 720B, China).

3. RESULTS AND DISCUSSION

Figure 2 exhibits the XRD patterns of NCM 622 (PDF#09-0063) and NCM 622-L samples. The specific unit cell parameters are shown in table 1. It is noted that all diffraction peaks belong to the α -NaFeO₂ structure and the space group is R $\bar{3}m$ [18]. The characteristic peak of La₂O₃ is not detected

because of the small amounts of coating. Obviously, the cell parameter values of the samples before and after coating are consistent with those reported in previous literatures [19], which indicates that La_2O_3 coating does not have a significant effect on the crystal structure. In general, all the material exhibits a good layered structure and a low degree of cation mixing because the $R (I_{(003)}/I_{(104)})$ is more than 1.2 [20]. The peaks of (006)/(102) and (108)/(110) are split clearly, which illustrates that all the samples display typical lamellar features [21].

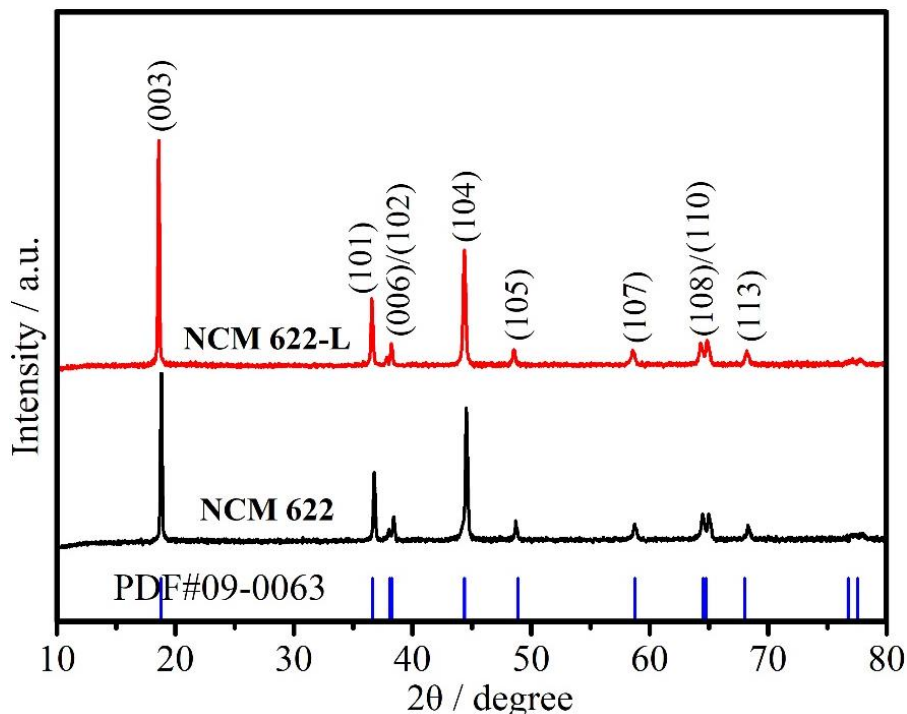


Figure 2. The XRD patterns of (a) NCM 622 and NCM 622-L

Table 1. Refined lattice parameters of NCM 622 and NCM 622-L

| Sample | a / (Å) | c / (Å) | c / a | $I_{(003)}/I_{(104)}$ |
|--------------|---------|---------|--------|-----------------------|
| The pristine | 2.853 | 14.234 | 4.9932 | 1.435 |
| 3.0-NCM 622 | 2.854 | 14.233 | 4.9887 | 1.474 |
| 5.0-NCM 622 | 2.857 | 14.241 | 4.9842 | 1.469 |

Figure 3 demonstrates the SEM images of NCM 622 and NCM 622-L. It can be seen from the figure that the NCM 622 samples before and after coating have an ellipsoidal shape with the secondary crystal grains around 5-15 μm . The size of the primary crystal grains reaches the nanoscale, indicating that the La_2O_3 coating does not affect the surface morphology of NCM 622. Compared with the uncoated samples, there are some small particles on the surface of NCM 622 after La_2O_3 coating, which reveals that the coating is successfully realized.

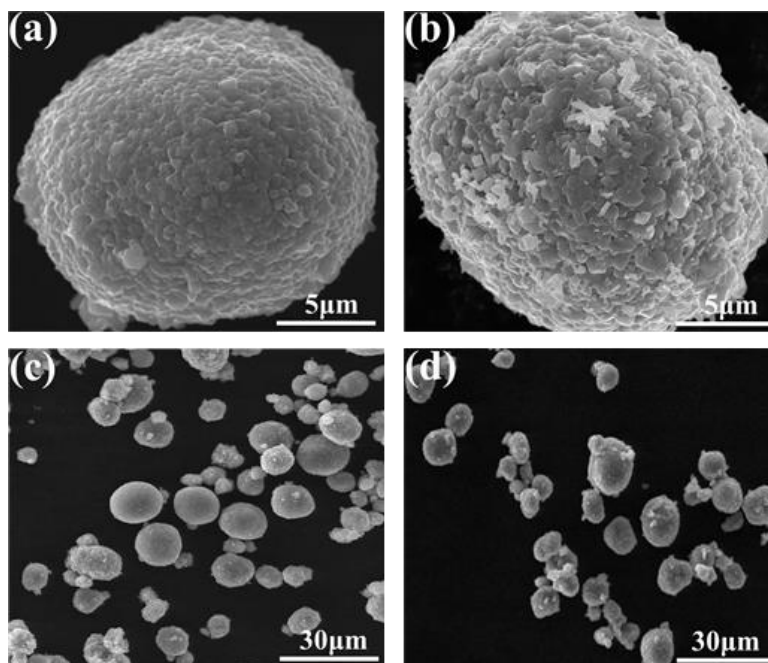


Figure 3. The SEM images of (a) NCM 622 and NCM 622-L

NCM 622-L is tested by energy dispersive spectrometer (EDS) to characterize the element types on the surface of NCM 622-L. As can be seen from Figure 4, the La element is distributed on the surface of the NCM 622. It can be seen from the Fig. 4(c), that the location of La are fully along with the substrate element Ni, Co and Mn, confirming the uniformly distribution of La_2O_3 in NCM 622-L sample.

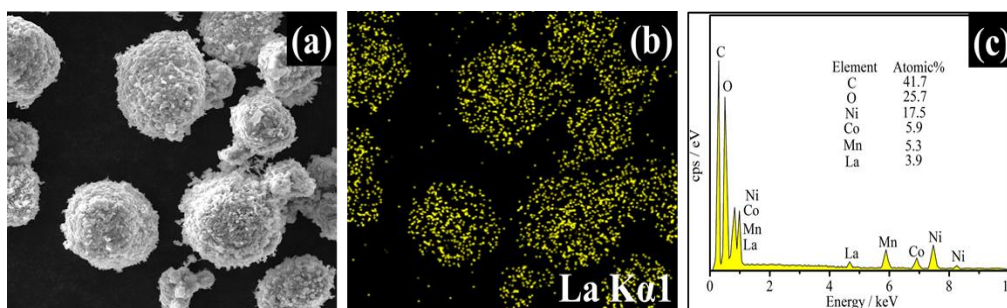


Figure 4. The EDS mappings of NCM 622-L

To further examine the effect of La_2O_3 coating on the electrochemical performance of NCM 622, the tests of initial charge/discharge and rate performance at 1 C ($1 \text{ C} = 180 \text{ mA} \cdot \text{g}^{-1}$) between 3.0 and 4.5 V at room temperature are presented in Figs. 5(a) and 5(b), respectively. It can be noticed from Fig. 5(a) that there is a voltage plateau around 3.8 V for the NCM 622 samples before and after coating. This process corresponds to $\text{Ni}^{4+} \leftrightarrow \text{Ni}^{2+}$ redox reaction [22]. The discharge capacity of NCM 622-L sample is slightly lower than bare one, it is may be because of the fact that La_2O_3 surface coating reduces the proportion of active material [23].

Figure 5(b) illustrates the rate performance of all the samples at 3.0-4.5 V. Noticeably, the discharge capacity of all the samples decreases with increasing rate. However, NCM 622-L displays higher capacities than NCM at all the rates tested. The capacity gap between the two samples becomes more prominent with the increase of discharge rate. The enhancement of the multiplying performance may be due to the good ionic conductivity of La_2O_3 , which improves the diffusion capacity of Li-ions between the electrode and the electrolyte interface. [24].

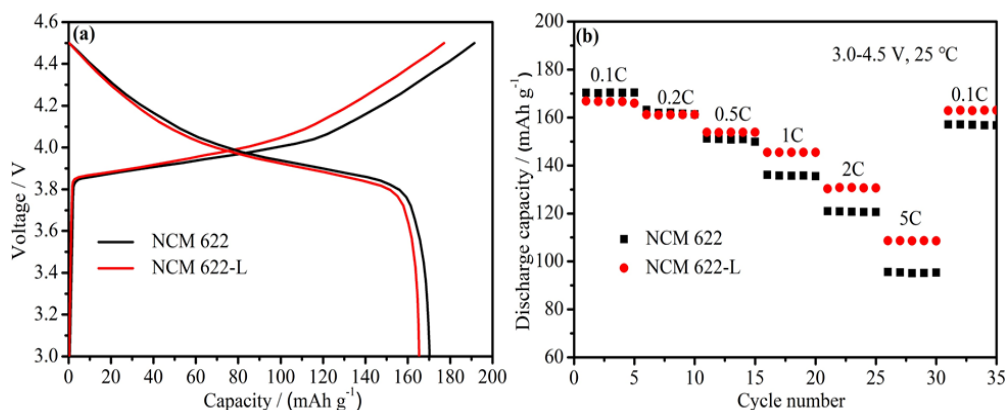


Figure 5. (a) Initial charge/discharge curves of NCM 622 and NCM 622-L at 0.1C. (b) Rate performance of NCM 622 and NCM 622-L at different current density

The cycling performance of all the samples after 100 cycles at 1 C discharge rate between 3.0 and 4.5 V at 25°C are shown in Figure 6(a). As expected, it can find the fact that the capacity retention of NCM 622-L (81.49%) is higher than that of NCM 622 (66.14%) after 100th cycles, which displays that the La_2O_3 coating can enhance the cycling performance of NCM 622 at the high cut-off voltage (4.5 V). In addition, the cycling performance of the two samples after 100 cycles at 1 C discharge rate between 3.0 and 4.3 V at normal cut-off voltage of 4.3 V are illustrated in Figure 6(b). The nano La_2O_3 coating can enhance the cycling performance of NCM 622 at normal cut-off voltage of 4.3 V. It is noted that the capacity retention of uncoated samples is 72.50%, while the NCM 622-L samples still maintained higher capacity retention (88.38%). To our best knowledge, the capacity fading of layered materials is primarily due to the side reaction between the active material and the electrolyte, and the degree of cation mixing be enhanced at high potential [25]. The surface coating could reduce the activity of active material by introducing strong La-O bonds on the surface of material, thereby reducing the surface reactivity of the active material with the electrolyte at high potential [26].

Figure 7 shows the CV curves of uncoated NCM 622 and NCM 622-L at the 1st, 3rd, and 5th cycles between 3.0 and 4.5 V with a scan rate of 0.1 mV/s. All samples process a couples of distinct redox peak in the 3.0-4.5 V range, which corresponds to the redox reaction of $\text{Ni}^{4+}/\text{Ni}^{2+}$ [27]. For the pristine NCM 622, the oxidation peak appears at 3.748 V in the 1st cycle, and this is related to the Li^+ de-intercalation process and to the oxidation of Ni^{2+} . The reduction peak appears at 3.689 V, which corresponds to Li^+ intercalation into the positive materials and the reduction of Ni^{4+} [28]. In accordance with previous reports, a smaller oxidation reduction gap ($\Delta E = E_{\text{oxidation}} - E_{\text{reduction}}$) means a less degree of electrode polarization [29]. The oxidation reduction gap (ΔE) of NCM 622 and NCM

622-L are shown in table 2. It can be seen that the ΔE of the NCM 622-L is significantly reduced after the La_2O_3 coating.

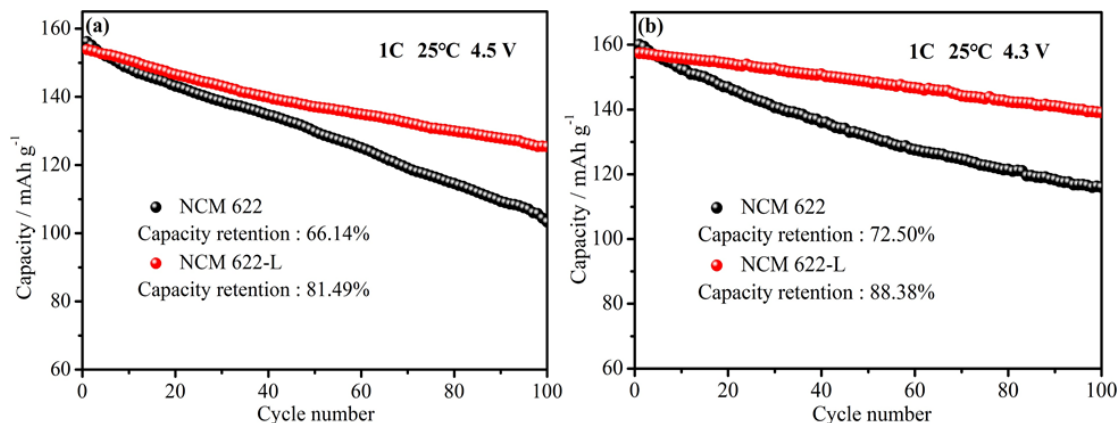


Figure 6. The cycling performance of NCM 622 and NCM 622-L (a) at 25 °C between 3.0 and 4.5 V and (b) between 3.0 and 4.3 V

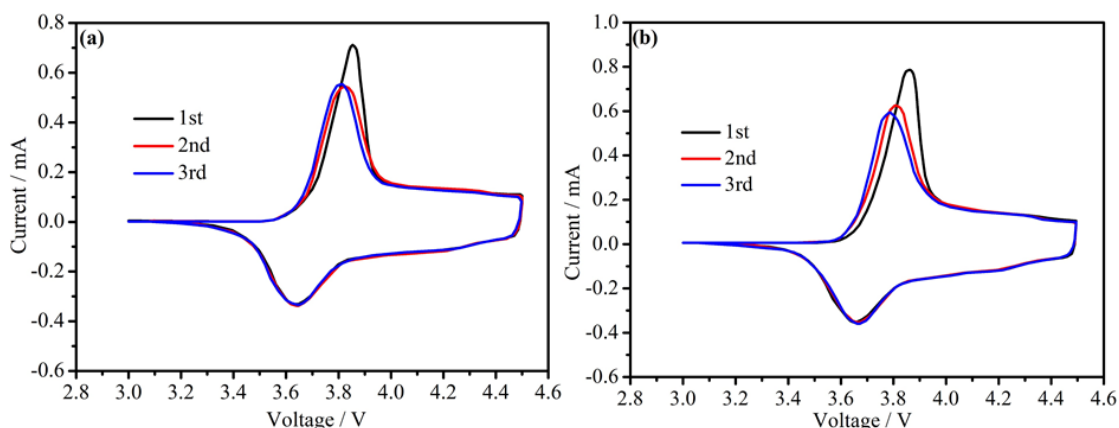


Figure 7. Cyclic voltammograms of (a) NCM 622 and (b) NCM 622-L

Table 2. The value of redox reaction gaps (ΔE)

| | Sample | 1st | 2nd | 3rd |
|---------------------|-----------|-------|-------|-------|
| redox reaction | NCM 622 | 0.218 | 0.175 | 0.166 |
| gaps (ΔE) | NCM 622-L | 0.196 | 0.136 | 0.115 |

In order to further studies the effect of La_2O_3 coating on the electrochemical performance of NCM 622, the electrochemical impedance tests of two electrodes are performed. The EIS curves of NCM 622 and NCM 622-L after 50 and 100 cycles are given in Figure 8, and the specific parameters are presented in Table 3. As can be seen from Figure 8 that the EIS curves of all samples consist of

semicircle in the high frequency region and oblique line in the low frequency region. The semicircle in the high frequency region is related to the charge transfer resistance (R_{ct}) [30]. The intercept of the semicircle with the real axis represents the electrolyte solution resistance of the working electrode (R_s) [31]. The oblique line in the low frequency region represents the Warburg impedance (W_o) describing Li^+ diffusion in the bulk material [32,33]. The fitted results are shown in Table 3, the NCM 622-L sample exhibit both smaller working electrode and transfer resistance This can be explained as follows: On the one hand, La_2O_3 coating can inhibits side reactions between electrolyte and active material to restrain the dissolution of the metal ions and give rise to protection of the NCM 622 particle from HF attack, which favors electron transfer. On the other hand, La_2O_3 shows favorable Li -ion conduction efficiency because it is a good lithium ion conducting medium. The results from EIS curves are consistent with the observation from rate performance from Figure 6.

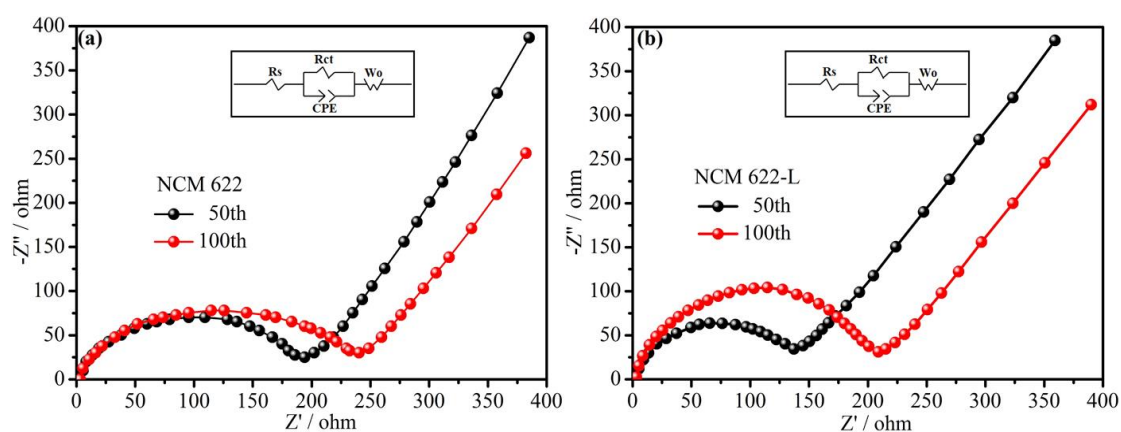


Figure 8. Nyquist curves of (a) the NCM 622 and (b) NCM 622-L after 50th and 100th at 25°C

Table 3. Impedance data of NCM 622 and NCM 622-L after different number of cycles at equilibrium state

| Cycling number | NCM 622 | | NCM 622-L | |
|----------------|------------|---------------|------------|---------------|
| | R_s /ohm | R_{ct} /ohm | R_s /ohm | R_{ct} /ohm |
| 50th | 2.951 | 183.6 | 2.465 | 109.4 |
| 100th | 3.298 | 295.4 | 2.469 | 188.6 |

4. CONCLISIONS

In this work, the NCM 622 positive material coated with La_2O_3 is successfully prepared by solvothermal method. Nano La_2O_3 skin on the NCM 622 core restrains the side reactions during cycling by separating the cathode materials from the electrolyte directly, which has been confirmed by SEM, EDS, CV and EIS analysis. As a result, the capacity retention of NCM 622-L after 100 cycles at a high cut-off voltage of 4.5 V is increased from 66.14% (uncoated NCM 622) to 81.49%. The EIS test results show that the impedance of the NCM 622-L sample is significantly reduced. Therefore, the La_2O_3 coating can effectively ameliorate the existing problem that excessive capacity fading of NCM

622 at high voltage. This facile coating method can also be applied to other layered transition-metal oxides to improved electrochemical performance of cathode materials.

ACKNOWLEDGEMENTS

Financial support from National Natural Science Foundation of China (No. 51764029, 51665022, and 51601081) are gratefully acknowledged.

References

1. W. Xiao, Z.Y. Nan, L. Cheng, Y.Z. Tao, Y.X. Hua, Z. Yi, Z.Z. Lin, *Int. J. Electrochem. Sci.*, 12 (2017) 12009.
2. Z.Y. Nan, D. Peng, Y.X. Hua, X.S. Biao, S.J. Jie, Y.R. Ming, L.H. Xin, S.Z. Zhong, Y. Yao, L. Xue, Z.Y. Jie, *Int. J. Electrochem. Sci.*, 12 (2017) 6853.
3. Z.Y. Nan, D. Peng, Z.M. Yu, S.X. Liang, Y.X. Hua, S.J. Jie, M. Qi, Li. Xue, Z.Y. Jie, *J. Appl. Electrochem.*, 48 (2017) 1.
4. B. Ying, C.Q. Jun, Y. Qi, Z. Sen, J. Kai, *Electrochim. Acta*, 112 (2013) 414.
5. G. Rui, S.P. Fei, C.X. Qun, S. Ling, *Electrochim. Acta*, 54 (2009) 5796.
6. L.L. Wei, D. Ke, P.Z. Dong, C.Y. Bing, H.G. Rong, *Chin. Chem. Lett.*, 25 (2014) 883.
7. H. Kaneda, Y. Koshika, T. Nakamura, H. Nagata, R. Ushio, K. Mori, *Int. J. Electrochem. Sci.*, 12 (2017) 4640.
8. L. Wen, W. Miao, G.X. Long, Z.W. Dong, C.J. Tao, Z.H. Hui, Z.X. Xiang, *J. Alloys Compd.*, 543 (2012) 181.
9. K.J. Zhou, R. Chong, T.G. An, Z. Xiang, L.A. Dong, W. Di, L. Hui, Z. Fei, *J. Power Sources*, 266 (2014) 433.
10. C. Chao, T. Tao, Q. Wen, Z. Hong, W. Ying, L. Bo, Y.Y. Bang, L.S. Guo, C. Ying, *J. Alloys Compd.*, 709 (2017) 708.
11. H.G. Rong, Z.M. Fang, W.L. Li, P.Z. Dong, D. Ke, C.Y. Bing, *J. Alloys Compd.*, 690 (2017) 589.
12. L.S. Jie, W. Hao, H. Ling, X.M. Wu, L. Heng, Z. Yun, *J. Alloys Compd.*, 674 (2016) 447.
13. T. Tao, C. Chao, Y.Y. Bang, L. Bo, L.S. Guo, C. Ying, *Ceram. Int.*, 43 (2017) 15173.
14. Q.C. Can, C.J. Li, C. Jun, D.G. Le, W.T. Fu, C.Y. Bin, T.Y. Feng, L.A. Dong, C.Y. Feng, *Dalton Trans.*, 45 (2016) 9669.
15. F.H. Qiang, L.S. Ying, Z.Z. Chang, W. Hua, S.Z. Cong, *Corros. Sci.*, 53 (2011) 3821.
16. F.H. Qiang, X.D. Hai, L.M. Cheng, L. Qian, *J. Alloys Compd.*, 702 (2017) 60.
17. Z. Lin, T.M. Jie, D.Y. Long, Z.Q. Ji, X.C. Gang, L.D. Min, *Ceram. Int.*, 14 (2016) 15623.
18. Y. Peng, W.Z. Xing, L.X. Hai, X.X. Hui, W.J. Xi, W.X. Wen, G.H. Jun, *Electrochim. Acta*, 95 (2013) 112.
19. Z.R. Rui, L.J. Xing, H.J. Jun, Z.R. Yu, Z.J. Feng, C.H. Yu, S. Guang, *J. Alloys Compd.*, 724 (2017) 1109.
20. Y. Kai, F.L. Zhen, G. Jia, Q.X. Hui, *Electrochim. Acta*, 63 (2012) 363.
21. L. Tao, L.X. Hai, W.Z. Xing, G.H. Jun, *J. Power Sources*, 342 (2017) 495.
22. H.G. Song, K.S. Park, Y.J. Park, *Solid State Ionics*, 225 (2012) 532.
23. L.X. Hui, K.L. Qin, S. Ting, L. Kun, C. Li, *J. Power Sources*, 267 (2014) 874.
24. H. Bin, L.X. Hai, W.Z. Xing, G.H. Jun, S. Li, W.J. Xi, *J. Power Sources*, 252 (2014) 200.
25. W.R. Heng, L.X. Hai, W.Z. Xing, G.H. Jun, W.J. Xi, *Electrochim. Acta*, 180 (2015) 815.
26. G.T. Fey, P. Muralidharan, L.C. Zhang, Y.D. Cho, *Solid State Ionics*, 176 (2015) 2759.
27. C.Y. Ping, Z. Yun, W. Fu, W.Z. Yi, Z. Qiang, *J. Alloys Compd.*, 611 (2014) 135.
28. Y.Z. Guang, G.X. Dong, X. Wei, H.W. Bo, Z. Jun, H.F. Rong, W. Kai, X. Yao, Z.B. He, *J. Alloys Compd.*, 699 (2017) 358.
29. K.S. Fei, Q.H. Fei, F. Yao, L. Xi, W.Y. Gang, *Electrochim. Acta*, 144 (2014) 22.

30. T.K. Fey, P. Muralidharan, L.C. Zhang, Y.D. Cho, *Electrochim. Acta*, 51 (2006) 4850.
31. Z.S. Zhe, Z. Hong, Z. Ti, Z.Z. Hui, L.P. Yu, R.L. Quan, *Corros. Sci.*, 67 (2013) 75.
32. C. Ho, I. Raistrick, R. Huggins, *J. Electrochem. Soc.*, 127 (1980) 343.
33. Z.Y. Nan, Z.Y. Jie, Z.M. Yu, X.M. Li, L. Xue, Y.X. Hua, D. Peng, *JOM*,
<https://doi.org/10.1007/s11837-018-2873-5>

© 2018 The Authors. Published by ESG (www.electrochemsci.org). This article is an open access article distributed under the terms and conditions of the Creative Commons Attribution license (<http://creativecommons.org/licenses/by/4.0/>).